RSC Advances

ROYAL SOCIETY OF CHEMISTRY

www.rsc.org/advances

Table of content:

An Exceptional Functionalization of Doped Fullerene Observed via Theoretical Studies on the Interactions of Sulfur-Doped Fullerenes with Halogens and Halides

Kayvan Saadata, Hossein Tavakol[a,*]

Interactions of sulfur-doped fullerenes with halogens and halides have been explored for possible applications such as sensor and adsorption processes.

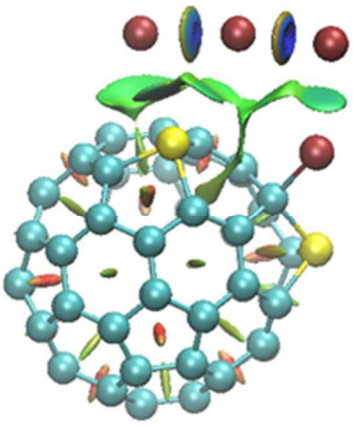

RSC Advances

ARTICLE

Received 00th January 20xx,
Accepted 00th January 20xx

DOI: 10.1039/x0xx00000x

www.rsc.org/

An Exceptional Functionalization of Doped Fullerene Observed via Theoretical Studies on the Interactions of Sulfur-Doped Fullerenes with Halogens and Halides

Kayvan Saadat[a], Hossein Tavakol[a,*]

This work reports study on the interactions of sulfur-doped fullerenes with halogens and halides (except iodine and iodide) to gain an enlightened vision to such interactions for employing them in possible applications such as sensor and surface adsorption. The ωB97XD DFT code has utilized in this study to obtain adsorption energies in the gas phase and solvent. The energy outcomes showed proper results for adsorptions in both gas and solvent (using PCM model). However, the gas phase interactions are more favorable thermodynamically. The formation of halide complexes releases more energy than the formation of halogen complexes and the strongest interaction is belong to the interactions of disulfur-doped fullerenes with halides. Donor-Acceptor transitions mostly affected by sulfur doping, which made C–S bond as auxiliary tool for the absorption process. The density of states (DOS) plots demonstrated better modification of conductivity properties upon sulfur-doping on fullerene structures. Electron densities and their Laplacians at bond critical points (BCPs) of interaction sites, NCI calculations and further visualizations proved the existence of such these interactions, clearly indeed. It's worthy to point that, in some cases, something like partial functionalization of fullerene have seen and these observations were approved via QTAIM, NCI and energy data. In these cases, the stable and thermodynamically favorable cation of halogenated doped fullerene (along with X_3^- as counter ion) could be produced from the interaction of double-doped fullerene with two molecular halogens.

[a] Department of Chemistry, Isfahan University of Technology, Isfahan 8415683111, Iran.

INTRODUCTION

After the first synthesis of fullerenes in 1985 by Smalley and Croto, new horizons have expanded in the chemistry of carbon nanomaterials.[1] Despite diamond and graphite, fullerenes are neutral, edgeless and have neither dangling bonds nor unpaired electrons. This would turn fullerenes to bearing unique properties such high-speed twirling around itself.[2] ARC discharge technique have been used as a main route for the synthesis of C_{60} and C_{70} fullerenes.[3,4] These molecules could be employed in superconductive materials,[5] organic electric conductors,[6] gas reservoir, gas separator, fuel cells and lubricants.[2] Tegos and coworkers were shown photosynthetic and antimicrobial properties of functionalized fullerenes by selective photodynamic treatment to produce active oxygen.[7] Although the mentioned applications of fullerenes are unique in case, the heterodoping of fullerenes gives them new potencies in electronic instruments, nanocomposites and sensors.[8,9] Wang and their colleagues reported a study on the adsorption process on $C_{35}B–H_2–C_{35}B$ (B-doped fullerene) from two directions. They observed barrierless H_2 bond breaking from physisorption toward chemisorption via 3D-potential energy curves.[10] In the case of sulfur-doping, Glenis et al. have succeeded in the synthesis of $C_{60-2n}S_n$, $C_{60-3n}S_n$ and $C_{60-4n}S_n$ fullerenes from thiophene using graphite electrode ARC discharge.[11] Moreover, density functional studies were employed to calculate the energies and structures of thiafullerenes in several oxidation states. The results predicted that $C_{59}S$ and $C_{59}S^{2+}$ is in closed-cage form and $C_{59}S^{4-}$ in opened-cage structure are the major forms among possible structures.[12] Sulfur-doping enhances the semiconductor behavior of CNTs, graphenes and fullerene.[13-16] The adsorption of molecular iodine on sulfur-doped fullerenes (SFs) via noncovalent interaction has reported using QTAIM and NBO analyses. This report has shown considerable transactions between iodine and S-doped fullerene that this type of interaction could be used in sensors.[16] Therefore, doped fullerenes are suitable candidate to employ in the adsorption of various molecules and prepare new sensors. The best tool to study of these interactions is computational chemistry, which could predict the existence and strength of noncovalent interaction precisely as well as its abilities to predict chemical properties, geometric structures and compounds specification.[17] Moreover, in these systems and using computational tools, three types of noncovalent interactions could be investigated, consisted of halogen bond (between X-X and S with the X-X...S angle near to 180 degrees), π-halogen bond (between halogen and π bond) and chalcogen bond

(between C-S and halide or halogen, halogen with 90 degrees angle and halogen is electron donor).[18-20] Therefore, in continuation of our previous studies in computational chemistry[21,22] and especially on the study of noncovalent interactions,[14-16] we have decided to attempt a full study of interactions of SFs with halogens and halides using appropriate DFT calculations. Because, despite several studies on the adsorption or sensor potencies of simple and doped fullerenes (or other nanostructures),[23-26] by reviewing the literature, any reports related to the interaction of halogens or halide anions with doped fullerenes have not been observed.

This study will be a guide to realize the interactions between SFs and halogens or halides (except iodine and iodide) and propose possible applications that might be take into advance in future for several purposes such as drug delivery, sensors, storages, etc. Moreover, QTAIM, NBO and NCI calculations were employed in addition to DFT calculations to provide more evidences about the natures and strengths of these interactions. Also we provide some evidence related to the functionalization (with halogen) of SFs in some special cases. Details of computations and the results obtained in this work are presented in the next sections.

METHODS

To start the simulation of noncovalent interaction between SFs and halogens or halides, we have optimized C_{60} fullerene and after geometry optimization, one and two sulfur atoms substituted permanently to result in $C_{59}S$ (SF) and $C_{58}S_2$ fullerenes (S2F1 and S2F2). The next step is to place molecular fluorine, chlorine and bromine (with code name X_2 (X=F, Cl and Br)) and halide anions (fluoride, chloride and bromide as X (X=F-, Cl- and Br-)) on the surfaces of doped fullerenes and optimize their structures. It should be pointed that in monosulfur-doping, the model name was set to SF and in disulfur-doping fullerenes, sulfur located approximately 90° and 180° from each other toward the center of fullerene sphere were respectively named as S2F1 and S2F2. Density Functional Theory (DFT) method has employed in this work because it vastly used to study of noncovalent interactions due to its lesser complexity against increasing system size, which is an advantage for DFT methods. Moreover, DFT calculations have been showed high abilities in the calculation of molecular properties[27,28] of chemical structures, comparable with the most computationally expensive MP2 methods,[29,30] and in prediction of thermodynamic and kinetic properties of chemical phenomena.[31,32] Among various DFT methods, ωB97XD have designed by Chai and Head-Gordon[33,34] as the best DFT code to interpret the intermolecular interactions because many DFT methods could not describe dispersive energy. This method is a development of former ωB97X method by applying some empirical correction for binary atomic dispersion.[35,36] After optimizations, the interaction energies for all complexes were calculated using Eq. 1.

$$\Delta E_{ads}=E_{complex}-(E_{absorbent}+E_{adsorbate}) \quad \text{Eq. 1}$$

Furthermore, to investigate the solvent effects, PCM model was take into advance to obtain solvation energies for every single optimized complex in benzene, chloroform and cyclohexane (three solvent with different polarities).[37] The Eq. 1 was employed to determine the interaction energies in solvents. All geometry optimizations and calculation of solvent effects were done using Gaussian 09 Revision A.01 suite[38] with ωB97X-D/6-31G level of theory. We used this nearly small basis set to decrease the calculation costs (because of using large systems) and more importantly, we have previously shown that there is not meaningful difference in the energy results when the level of basis set increased in DFT calculations.[39]

Regarding to the valuable work of Weinhold et al. on introducing NBO concepts, this calculation was also performed on each optimized structure to yield accurate atomic charges and donor-acceptor transactions of SFs with halogens and halides via NBO 3.1, integrated in Gaussian 09 program.[40] To monitor the changes in conductive levels of SFs, density of states (DOS) plots were depicted by utilizing GaussSum software.[41] To calculate reactivity parameters, Koopman's theorem[42] was employed to obtain chemical potential (μ), chemical hardness (η), global softness (S) and electrophilicity index (ω) for all complexes from the following equations.

$$\mu=(E_{LUMO}+E_{HOMO})/2 \quad \text{Eq. 2}$$

$$\eta=(E_{LUMO}-E_{HOMO})/2 \quad \text{Eq. 3}$$

$$S=1/\eta \quad \text{Eq. 4}$$

$$\omega=\mu^2/2\eta \quad \text{Eq. 5}$$

Bader's quantum theory of atoms in molecules (QTAIM),[43] were employed to calculate the electron densities and Laplacians of electron densities at bond critical points (BCPs) in noncovalent interaction sites using AIMAll program.[44] Finally, based on the interesting works of Johnson, Conterares-Garcia and their colleagues on noncovalent interaction (NCI) indexes, it seems strongly indispensable to perform this calculation in current research as well. The NCI indexes are related to the fundamental dimensionless parameter in DFT, called reduced density gradient (RDG), as described by S parameter in Eq. 6.

$$s=\frac{1}{2(3\pi^2)^{1/3}}\frac{|\nabla\rho|}{\rho^{4/3}} \quad \text{Eq. 6}$$

Since the sign of λ2 is proportional to the essence of the interactions, the plots consisted of sign of λ2×ρ versus RDG would indicate a noncovalent interaction near zero area (horizontal axis).[45] To fulfil this, the wavefunctions obtained from the optimized structure for each complex has been examined by NCIPLOT program[46] and depicted using VMD 1.9.1 software,[47] in which the green color in isosurfaces means a weak and noncovalent interaction between SFs and halogen or halides. The plots of sign λ_2×ρ versus RDG have been drawn by gnuplot 4.6.5.[48]

RESULT AND DISCUSSION

Optimized structures

The first step of this work is the optimization of three doped fullerenes (SF, S2F1 and S2F2) to consider their interactions

with halogens and halides. The optimized structures of these three initial structures (or adsorbents, generally names as SFs) were shown in Fig. 1. Then, they was interacted with six molecule (three halides and three molecular halogens) as adsorbates, i.e. F^-, Cl^-, Br^-, F_2, Cl_2 and Br_2. For complexes with the molecular halogens, it is possible to consider two different situations of halogens versus SFs, one is direct (the angle of SF-X-X is near to 180 degrees that could has halogen bond) and another is perpendicular (the angle of SF-X-X is near to 90 degrees that could has π-halogen or chalcogen bond). It is noticeable that in complexes with halide anions, mostly chalcogen bond could be existed.

Fig. 1 The optimized structures of Mono and disulfur-doped fullerene as employed adsorbents in the calculations

Therefore, for complex between SF and each molecular halogens, two different configurations could be considered i.e. direct position or SF-D-X_2 and perpendicular position or SF-P-X_2. Although, for complexes of S2F1 (or S2F2) with each molecular halogens, three different configurations could be considered i.e. direct position of both halogens or S2F1-2D-X_2, perpendicular position of both halogens or S2F1-2P-X_2 and direct position of one halogen with perpendicular position of another halogen or S2F1-DP-X_2. Therefore, total 33 complexes between SFs and halogens or halides were considered and their structures were optimized. The optimized structures of these complexes were depicted in figures 2-4, respectively for SF, S2F1 and S2F2 complexes. In these figures, the minimum distance between absorbent and adsorbate has been mentioned for each complex.

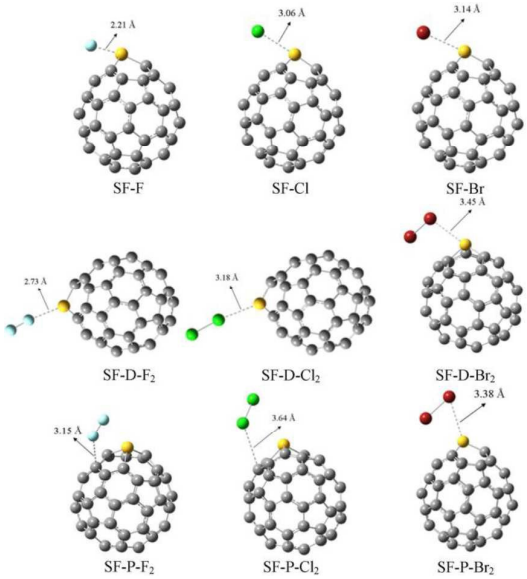

Fig. 2 The optimized structures for noncovalent complexes of monosulfur-doped fullerene (SF) with halogens and halides

The average C–S bond lengths in SFs (obtained from the calculations) are 1.864Å and 1.863Å, respectively for single and double doping. In the complexes with halogens, direct positions with halogen bond have the less SF…X distance versus the perpendicular positions with chalcogen or π-halogen bonds.

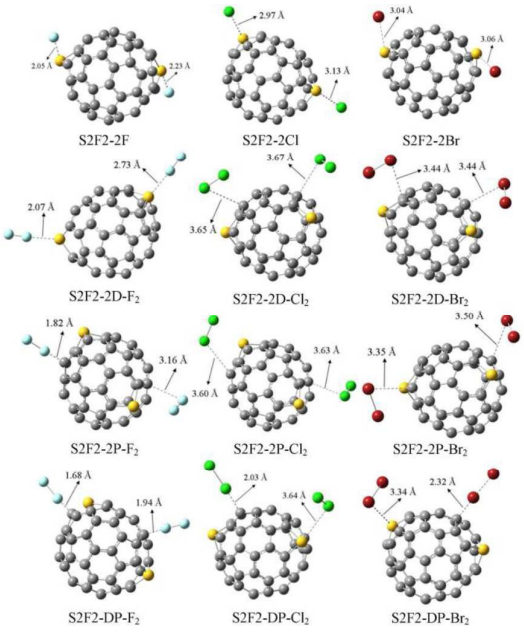

Fig. 3 The optimized structures for noncovalent complexes of S2F1 (first disulfur-doped fullerene) with halogens and halides

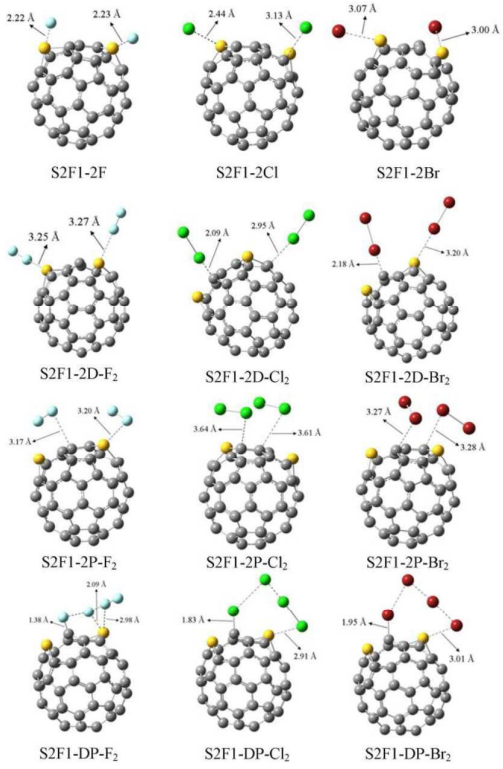

Fig. 4 The optimized structures for noncovalent complexes of S2F2 (another disulfur-doped fullerene) with halogens and halides

Expected structural deviation from the normal spherical form of fullerene has been seen in doped sulfur sites. Noticeably, it was found that despite the initial situation of each model, some complexes have changed from direct mode into perpendicular situation or reverse after optimization process. Examples are SF-D-Br_2, S2F2-2D-Cl_2, S2F2-2D-Br_2 and all S2F1-DP and S2F2-DP models. Two later cases showed unusually geometrical parameters as such small interatomic distances between one halogen atom and carbon atom next to the dopant sulfur. These cases could be considered as partial functionalization and will be discussed from the energy and QTAIM point of view in the following sections. Apparently, all minimum distances between absorbent and adsorbates (except functionalization cases) were between 1.8-3.7 Å. Therefore, these interactions could be classified as noncovalent interaction definitions from what Cerny and Hobza expressed about distance of noncovalent interaction point of view.[49] As a general comparison, it should be mentioned that typically these distances are in the lowest magnitude for fluorine-bearing complexes. In DP models, the lowest distances have been observed in S2F1-DP models that one halogen atom was located on covalent distance of the carbon atom next to the doped sulfur atom. Furthermore, other data help us to explain such happening.

Interactions energies in the gas and solvent

In order to determine the possibility and strength of the interactions, the adsorption energies of halogens and halides on the surfaces of SFs for various possible configurations of each model in the gas phase and three solvents (benzene, chloroform and cyclohexane) were calculated according to Eq. 1 and the results were provided in Table 1.

The calculated results showed thermodynamically desirable energies for all noncovalent interaction in both gas and solvent phases. Generally, adsorption of halides are more favorable than molecular halogens by noticeable values. For the interactions with halide, more noncovalent interaction energy released with the order of fluoride>bromide>chloride and maximum interaction energy calculated for S2F2-2F model with 104.56 kcal/mol. Although, double doping complexes have adsorption energies slightly less than twice versus the single doped complexes. This means that the relation between adsorption energy and the number of dopant is not completely linear. In the solvent, the most stability is belonging to fluoride complexes and in all halide complexes, cyclohexane is the solvent with the highest released interaction energies. This could be assigned to the lesser polarity of complexes when they take interactions together versus when the complex parts stay individual in the solvent. Therefore, the interaction of each halide typically was more powerful than that of molecular halogen analogues. It could be concluded that chalcogen bond (existed in halide complexes) has more strength than halogen bond (existed in direct halogen complexes) and π-halogen bond.

In the interactions of halogens with SFs, we keep an eyes to SF-D and SF-P models. As long as bromine molecule was stay perpendicular to the fullerene's surface, it could be deduced that interactions those which halogen molecule stands perpendicularly above the fullerene have much stability toward directly situated ones and is correct generally for S2F1-2P and S2F1-2D models as well. In other words, bromine prefers chalcogen or π-halogen bond than halogen bond. For chlorine and bromine, noncovalent interactions with S2F1 are more favorable than S2F2, but for fluorine case this is reverse. Moreover, in complexes with one molecular halogen, perpendicular positions have more negative interaction energies that shows the preferability of π-halogen or chalcogen bond versus halogen bond in these systems.

More importantly, an interesting observation was happened for S2F1-DP model in which a large number of stabilization energy has been calculated that it is not acceptable to sort them out into noncovalent interaction classification. In these complexes, the energy values up to 3 times larger than other analogues models, higher interaction energies in the solvent (opposite to observed orders in the other complexes) and small distances between halogen atom and neighboring carbon atom of sulfur dopant tell us a new story beyond a simple noncovalent interaction. In these cases, it seems that SFs have functionalized by halogens and we have $[SF\text{-}X]^+X_3^-$. This type of functionalization could be interesting and useful in the future researches regard to the chemistry of doped fullerenes. However, more quantum mechanics-based analyses are needed to confirm this observation and we wish to provide them in the next sections.

Table 1. Interaction energies of all complexes in the gas and solvents (benzene, chloroform and cyclohexane)

ΔE_{ads}	Gas	Benzene	Chloroform	Cyclohexane
SF-F	-77.31	-46.40	-34.32	-49.39
SF-Cl	-28.68	-10.42	-4.22	-12.06
SF-Br	-32.81	-14.97	-8.74	-16.59
SF-D-F_2	-1.14	-1.02	-0.95	-1.04
SF-D-Cl_2	-1.15	-1.04	-0.95	-1.06
SF-D-Br_2	-7.48	-7.46	-7.37	-7.47
SF-P-F_2	-2.41	-2.31	-2.23	-2.32
SF-P-Cl_2	-2.19	-2.07	-1.99	-2.09
SF-P-Br_2	-7.43	-7.21	-7.08	-7.23
S2F1-2F	-93.99	-64.01	-52.85	-66.84
S2F1-2Cl	-8.54	0.51	2.14	-0.10
S2F1-2Br	-14.06	-7.48	-6.93	-7.85
S2F1-2D-F_2	-0.30	-0.02	0.07	-0.04
S2F1-2D-Cl_2	-21.76	-30.04	-35.21	-28.99
S2F1-2D-Br_2	-26.97	-33.16	-37.22	-32.36
S2F1-2P-F_2	-5.01	-4.82	-4.69	-4.84
S2F1-2P-Cl_2	-6.42	-6.21	-6.09	-6.24
S2F1-2P-Br_2	-20.77	-20.18	-19.77	-20.26
S2F1-DP-F_2	-94.13	-97.38	-99.47	-96.96
S2F1-DP-Cl_2	-52.87	-60.79	-65.27	-59.85
S2F1-DP-Br_2	-62.82	-68.41	-71.69	-67.73
S2F2-2F	-104.56	-73.02	-60.75	-76.07
S2F2-2Cl	-14.39	-4.54	-2.24	-5.28
S2F2-2Br	-20.91	-12.41	-10.50	-13.04
S2F2-2D-F_2	-2.79	-2.72	-2.67	-2.74
S2F2-2D-Cl_2	-5.62	-5.60	-5.54	-5.61

S2F2-2D-Br_2	-15.21	-14.73	-14.56	-14.76
S2F2-2P-F_2	-9.92	-14.73	-17.85	-14.11
S2F2-2P-Cl_2	-5.69	-5.31	-5.12	-5.34
S2F2-2P-Br_2	-16.22	-15.88	-15.63	-15.93
S2F2-DP-F_2	-22.62	-33.61	-40.56	-32.22
S2F2-DP-Cl_2	-12.30	-16.42	-19.21	-15.88
S2F2-DP-Br_2	-22.53	-26.21	-28.72	-25.72

NBO Analyses

NBO calculations have been executed to obtain some useful information about the interactions. Two main categories of data obtained from the NBO calculations that are atomic charges and donor-acceptor transaction (E_2 interaction energies). Table 2 charted the selected important atomic charges involved in the noncovalent interactions of SF complexes (only for fullerene doped with one sulfur atom) along with the SF alone and the full results of NBO atomic charges could be observed in supporting information (Table S1). In Table 2, the average of atomic charges of three carbon atoms connected to the doped sulfur atom was reported as C (Av) charge, the charge of doped sulfur atom was reported as S charge and the charges of halogen atom(s) (one atom for halide complexes and two atoms for halogen complexes) were reported as X(1) (the closer halogen atom) and X(2).

Table 2. Selected NBO atomic charges for complexes of SF with halogens and halides

Complexes	S	C (Av)[a]	X(1)	X(2)
SF (alone)	0.859	-0.198	-	-
SF-F	0.977	-0.178	-0.731	-
SF-Cl	0.934	-0.171	-0.866	-
SF-Br	0.918	-0.173	-0.820	-
SF-D-F_2	0.871	-0.197	-0.026	-0.010
SF-D-Cl_2	0.853	-0.194	-0.028	-0.004
SF-D-Br_2	0.856	-0.196	-0.007	0.018
SF-P-F_2	0.860	-0.197	-0.003	0.006
SF-P-Cl_2	0.857	-0.196	-0.005	0.007
SF-P-Br_2	0.852	-0.197	0.000	0.013

[a] This value is the average of atomic charges of three carbon atoms connected to the doped sulfur

According to the atomic charge data, the negative charges (for halogen atom) in all noncovalent interaction are in this order: chloride>bromide>fluoride. This means that fluoride transfers more negative charge to SFs versus other halides. These values are in accordance with the calculated adsorption energies, which showed the fluoride has the best interaction (and the maximum charge transfer) and chloride has the worse interaction (and the minimum charge transfer) in our models. Moreover, the alteration of atomic charge of SFs (versus the SF alone) in halide complexes is more than that in halogen complexes. For example, the S charge in SF, SF-F, SF-D-F_2 and SF-P-F_2 are respectively 0.859, 0.977, 0.871 and 0.860 au. The same conditions could be observed for the C (Av) charges.

In complexes with halogens (molecular), for halogens connected directly to the fullerene, much more atomic charge has been observed in contrast with those staying perpendicularly. This could be seen in SF-D-X_2 and SF-P-X_2 (X=F,Cl) models while in bromine complexes, they are perpendicular in both modes and they had more positive charges compared with fluorine and chlorine complexes. It's noticeable that for S2F1-DP-X_2 (X=F,Cl,Br) and S2F2-DP-X_2 (with lesser extent), an inharmonic rhythm has been found out especially for atomic charge of carbon atoms next to doped sulfur atom. Therefore, more negative charges has been observed for halogen atoms in contrast with other 2D or 2P analogue models.

Table 3 presents the strongest second order perturbation energies for donor-acceptor transactions of each model. In halide complexes, in agreement with previous results, the fluoride has the highest E_2 interaction energies while in halogen complexes, there is not meaningful relation between the kind of halogen and E_2 energies. In the most of interactions, the lone-pair of halogen acts as electron donor and C–S antibonding sigma bond ($\sigma^*_{C\text{-}S}$) acts as electron acceptor, which could be a referral to role of S-doping in driving transactions in such manner. Moreover, except in some cases, the π-bond is not participated as donor or acceptor in these interactions. These observations show that in perpendicular positions, chalcogen bond plays a major role in these interactions. However, in models consisted of direct configuration of halogens versus SFs (except bromine complexes which stay perpendicular in both), the transaction could be observed from the lone-pair of doped-sulfur to X–X antibonding. Noticeably, some complexes such as S2F1-2D-Br_2 and S2F2-DP-X_2 (X=F, Cl, Br) show the huge amount of E2 energies in their electron transfers from the lone-pair of carbon atom (next to dopant sulfur) to of σ^* halogens. In a few cases (S2F1-2D-Cl_2 and S2F2-2P-F_2), one halogen atom is so closed to the carbon that made them as a unified acceptor group and also very strong transitions were observed for them. Finally, for S2F1-DP-X2 (X=F, Cl, Br) models, $LP_X \rightarrow \sigma^*_{C\text{–}S}$ transitions has more energy values in contrast with the similar transitions in other models.

Table 3. The strongest second order perturbation energies (E2) of donor-acceptor transactions for selected complexes

Complex	Donor	Acceptor	E_2[a]
SF-F	LP F	σ* C-S	37.09
SF-Cl	LP Cl	σ* C-S	9.01
SF-Br	LP Br	σ* C-S	8.82
SF-D-F_2	LP S	σ* F-F	2.97
SF-D-Cl_2	LP S	σ* Cl-Cl	3.30
SF-D-Br_2	LP Br	σ* C-S	2.45
SF-P-F_2	LP F	σ* C-S	0.65
SF-P-Cl_2	LP Cl	σ* C-S	0.87
SF-P-Br_2	LP Br	σ* C-S	2.89
S2F1-2F	LP F	σ* C-S	35.71
S2F1-2Cl	LP Cl	π* C-C	10.78
S2F1-2Br	LP Br	σ* C-S	22.28
S2F1-2D-F_2	LP F	σ* C-S	0.48
S2F1-2D-Cl_2	LP Cl	σ* C-Cl	117.57
S2F1-2D-Br_2	LP C	σ* Br-Br	239.28
S2F1-2P-F_2	LP F	σ* C-S	0.95
S2F1-2P-Cl_2	LP Cl	σ* C-S	0.40
S2F1-2P-Br_2	LP C	σ* Br-Br	4.53
S2F1-DP-F_2	LP F	σ* C-S	45.34
S2F1-DP-Cl_2	LP Cl	σ* C-S	16.41
S2F1-DP-Br_2	LP Br	σ* C-S	16.17
S2F2-2F	LP F	σ* C-S	64.40
S2F2-2Cl	LP Cl	σ* C-S	16.20
S2F2-2Br	LP Br	σ* C-S	19.21

S2F2-2D-F_2	LP S	σ* F-F	3.47
S2F2-2D-Cl_2	LP Cl	π* C-C	0.25
S2F2-2D-Br_2	LP Br	σ* C-S	2.48
S2F2-2P-F_2	LP F	σ* C-F	123.56
S2F2-2P-Cl_2	LP Cl	σ* C-S	0.93
S2F2-2P-Br_2	LP Br	σ* C-S	3.35
S2F2-DP-F_2	LP C	σ* F-F	204.29
S2F2-DP-Cl_2	LP C	σ* Cl-Cl	172.70
S2F2-DP-Br_2	LP C	σ* Br-Br	165.70

[a]All values are in Kcal/mol.

Population analyses and DOS plots

To realize the sensor behavior of SFs, probing onto HOMO and LUMO energies and their energy gaps, it seems essential to obtain some reactivity indexes from the equations 2 to 5 to describe changing the chemical behavior upon S-doping. Table 4 has provided HOMO and LUMO energy values, their energy gaps, chemical potential, chemical hardness, chemical softness and electrophilicity indexes of fullerene (C_{60}) and employed SFs to compare the behavior of fullerene after sulfur-doping. In addition, to get more insight about the electronic properties of these structures, Figure 5 shows the DOS plots for each of them (C_{60} and SFs).

As it's determined, C_{60} fullerenes has a high E_g value versus SFs and upon doping, the Eg value reduces that this decrease will be larger when the number of adjacent dopant atoms increases. Moreover, the HOMO energy level shifts up (to more positive values) upon doping that means increasing in nucleophilicity or electron donation property and LUMO energy reduced a little (to more negative values) that means the decreasing in electrophilicity indexes (this value will be confirmed by the electrophilicity index at last column).

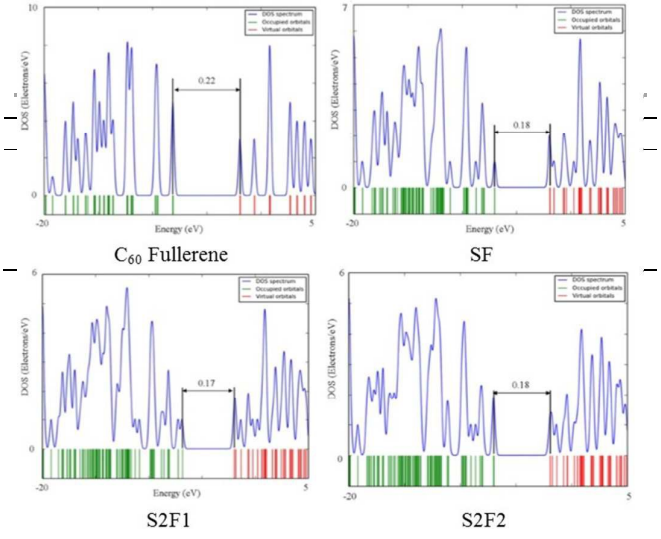

Fig. 5 DOS plots of fullerene and SFs (HOMO and LUMO levels are indicated by narrow bar. Energy gap dimensions are in eV

These values show the reduced reactivities (and increasing in stability) of fullerene after doping that they confirmed by the chemical potential (μ) values listed at the 5th column. Observed E_g values for SF and S2F2 are similar to each other but for S2F1 fullerene, lesser E_g gap has been revealed. Obtained results has been stated a modification of electronic properties due to sulfur doping of fullerenes in about 18% to 20%. Surely, the chemical hardness decreases and global softness increases by sulfur doping of C_{60} fullerene. All of these values confirm the distinct change in the behavior of SFs versus simple fullerenes and everyone could use them by desired manner to obtain the better results.

QTAIM analyses and NCI indexes

As mentioned before, the electron density (ρ) and its Laplacian ($\nabla^2\rho$) at BCPs of noncovalent interaction sites could ensure the existence of this kind of interaction and also determine what they are actually in characteristic. After performing QTAIM calculation, ρ and $\nabla^2\rho$ values from those BCPs which desired on interaction area were extracted. Table 5 presented the important data of electron densities and their Laplacians at BCPs in noncovalent interaction sites between SFs and halogens or halides. In some cases, more than one critical point was observed for each complex. In addition, a unique picture of noncovalent interaction for each case with clarifying that green and red dots on pictures represented as BCPs and RCPs (Ring Critical Point) were shown in supporting information (Figure S1-S3).

It was obviously found that electron densities in critical points of halide complexes are much higher than those in halogen complexes. Regard to this, for fluoride complexes, F–S and F–C interactions have the highest ρ values among observed BCPs in SF and S2F2 complexes. In chloride cases, the interactions labeled with Cl–S and Cl–C have the maximum ρ values in S2F1 and S2F2 interactions, respectively. Although, Br–S and Br–C interactions have the highest ρ values in their BCPs in S2F2 and SF complexes. The high magnitude and positive sign of the electron density's Laplacian in BCPs indicates electrostatic (noncovalent) essence of these interactions. For S2F1-DP-X_2 (X=F, Cl, Br) complexes that will described separately, interaction of molecular fluorine with S2F2 has the highest ρ values in both F–S and F–C interactions.

Moreover, in SF and S2F1 complexes, Cl–S and Cl–C interactions respectively have the largest ρ values in their BCPs for chlorine complexes. At last, for bromine complexes, both Br–S and Br–C have the maximum magnitude of ρ in BCPs by interaction with S2F1. All mentioned complexes above, have positive Laplacian of ρ at BCPs, which illustrate electrostatic interaction occur through this procedure.

However, something special was observed in S2F1-DP-X_2 (X= F, Cl, Br) complexes in which some ρ values and the sign of their

Laplacian would make us suspecting that it is not a formal noncovalent interaction. The ρ values for X–C (X=F, Cl, Br) interactions were 0.2325, 0.1492, and 0.1338 e/a_o^3 respectively for fluorine, chlorine and bromine. Apparently, these values are not in the range of other complexes that bearing electrostatic noncovalent interaction. This will be approved when we observe negative sign for Laplacian of ρ value in relative BCPs that is -0.2841, -0.0576 and -0.0451 e/a_o^5 respectively for fluorine, chlorine and bromine. Table 6 will brought an extended version of all BCP near interaction sites for all S2F1-DP complexes to give additional insight for understanding this phenomenon. As it could be seen from the above table, the carbon next to doped sulfur atom seems to have covalent bond with one halogen atom due to negative Laplacian of ρ at given BCP. According to these data, a comparison between ρ values of C–S BCPs indicates the reduced covalent strength of one C–S bond. With respect to this fact, since two halogen atoms have interaction with SF either covalently or noncovalently, two remain halogen atoms have some kind of secondary interaction that is notable in magnitude (for F–F, Cl–Cl and likely Br–Br). Therefore, the low distance between halogens and SF will lead us a partial functionalization (halogenation) of S2F1 and we have the stable structure as $[S2F1\text{-}X]^+X_3^-$ produced from S2F1 and two molecular halogens via exothermic process. Take a more precise look on the results of diminished C–S BCP's ρ values for fluorine, chlorine and bromine reveal this fact that fluorine would reduce the strength of C–S bond more than chlorine and bromine.

Table 5. Electron densities (ρ) and their Laplacian ($\nabla^2\rho$) of important BCPs at noncovalent interaction sites for all complexes obtained from the QTAIM calculations

$\nabla^2\rho(e/a_o^5)$	$\rho(e/a_o^3)$	Type	Complex	$\nabla^2\rho(e/a_o^5)$	$\rho(e/a_o^3)$	Type	Complex	$\nabla^2\rho(e/a_o^5)$	$\rho(e/a_o^3)$	Type	Complex
S2F1-2F	F–S	5.5E-02	1.8E-01	S2F2-DP-Cl_2	Cl–C	5.7E-02	1.1E-01	SF-P-Br_2	Br–S	1.1E-02	3.8E-02
	F–S	5.4E-02	1.8E-01		Cl–S	4.9E-03	1.9E-02		H–C	8.1E-03	2.7E-02
S2F1-2Cl	Cl–C	1.9E-02	5.4E-02		Cl–C	4.3E-03	1.4E-02	S2F1-2D-F_2	F–S	4.7E-03	2.3E-02
	Cl–S	1.6E-02	5.3E-02		Cl–C	3.3E-03	1.1E-02		F–S	4.2E-03	2.2E-02
S2F1-2Br	Br–S	2.5E-02	6.7E-02	S2F2-DP-Br_2	Br–C	6.3E-02	9.6E-02	S2F1-2D-Cl_2	Cl–C	9.3E-02	1.1E-01
	Br–S	2.2E-02	6.0E-02		Br–S	1.1E-02	4.0E-02		Cl–C	1.4E-02	5.0E-02
S2F2-2D-F_2	F–S	1.9E-02	7.7E-02		Br–C	7.5E-03	2.2E-02	S2F1-2D-Br_2	Br–C	8.7E-02	8.8E-02
	F–S	1.2E-02	7.2E-02		Br–S	7.4E-03	2.7E-02		Br–S	1.3E-02	4.8E-02
S2F2-2D-Cl_2	Cl–C	4.6E-03	1.5E-02	S2F2-2F	F–S	7.7E-02	2.3E-01	S2F1-2P-F_2	F–S	5.9E-03	3.0E-02
	Cl–C	4.1E-03	1.4E-02		F–S	5.5E-02	1.8E-01		F–C	4.1E-03	1.9E-02
	Cl–C	4.6E-03	1.5E-02	S2F2-2Cl	Cl–S	2.2E-02	6.6E-02		F–C	4.0E-03	1.9E-02
	Cl–C	4.3E-03	1.4E-02		Cl–S	1.6E-02	5.2E-02		F–C	4.7E-03	2.2E-02
S2F2-2D-Br_2	Br–S	9.6E-03	3.3E-02		Cl–C	8.9E-03	2.7E-02		F–C	4.7E-03	2.2E-02
	Br–C	8.1E-03	2.5E-02	S2F2-2Br	Br–S	2.3E-02	6.3E-02		F–S	4.4E-03	2.4E-02
	Br–C	6.2E-03	1.9E-02		Br–C	2.2E-02	6.0E-02	S2F1-2P-Cl_2	Cl–C	5.2E-03	1.6E-02
	Br–S	9.5E-03	3.2E-02	SF-F	F–S	5.7E-02	1.9E-01		Cl–C	4.4E-03	1.4E-02
	Br–C	8.2E-03	2.5E-02		F–C	2.3E-02	9.8E-02		Cl–C	4.8E-03	1.5E-02
	Br–C	6.0E-03	1.9E-02		F–C	2.3E-02	9.8E-02		Cl–C	4.6E-03	1.5E-02
S2F2-2P-F_2	F–C	9.3E-02	2.5E-01	SF-Cl	Cl–S	1.9E-02	5.8E-02	S2F1-2P-Br_2	Br–C	1.2E-02	3.7E-02
	F–S	6.1E-03	3.0E-02		Cl–C	1.2E-02	4.0E-02		Br–S	1.2E-02	4.2E-02
	F–C	5.3E-03	2.4E-02	SF-Br	Br–S	1.9E-02	5.5E-02		Br–C	1.1E-02	3.3E-02
S2F2-2P-Cl_2	Cl–C	5.0E-03	1.6E-02		Br–C	1.5E-02	4.6E-02		Br–C	1.1E-02	3.5E-02
	Cl–S	4.7E-03	1.8E-02	SF-D-F_2	F–S	1.8E-02	4.7E-02		Br–S	9.8E-03	3.5E-02
	Cl–C	4.5E-03	1.5E-02	SF-D-Cl_2	Cl–S	1.2E-02	1.5E-02		Br–S	7.1E-03	2.5E-02
	Cl–C	4.5E-03	1.5E-02	SF-D-Br_2	Br–S	9.6E-03	3.3E-02		Br–C	6.7E-03	1.9E-02
S2F2-2P-Br_2	Br–S	1.1E-02	3.9E-02		Br–C	8.0E-03	2.5E-02	S2F1-DP-F_2	F–C	2.3E-01	-2.8E-01
	Br–S	7.7E-03	2.8E-02		Br–C	6.3E-03	2.0E-02		F–S	7.1E-02	2.3E-01
	Br–C	7.5E-03	2.8E-02	SF-P-F_2	F–C	5.5E-03	2.4E-02	S2F1-DP-Cl_2	Cl–C	1.5E-01	-5.8E-02
	Br–S	9.3E-03	3.2E-02		F–S	4.8E-03	2.7E-02		Cl–S	2.4E-02	7.3E-02
	Br–C	8.0E-03	2.5E-02		F–S	4.1E-03	2.3E-02	S2F1-DP-Br_2	Br–C	1.3E-01	-4.5E-02
S2F2-DP-F_2	F–C	1.3E-01	2.9E-01	SF-P-Cl_2	Cl–S	4.9E-03	1.9E-02		Br–S	2.4E-02	6.7E-02
	F–C	7.0E-02	2.2E-01		Cl–C	4.5E-03	1.4E-02		Br–S	1.2E-02	4.3E-02

Table 6. Electron densities (ρ) and their Laplacian ($\nabla^2\rho$) of important BCPs for partial functionalized S2F1-DP-X_2 (X=F, Cl, Br) complexes

S2F1-DP-F_2			S2F1-DP-Cl_2			S2F1-DP-Br_2		
Type	$\rho(e/a_o^3)$	$\nabla^2\rho(e/a_o^5)$	Type	$\rho(e/a_o^3)$	$\nabla^2\rho(e/a_o^5)$	Type	$\rho(e/a_o^3)$	$\nabla^2\rho(e/a_o^5)$
F–F	0.1792	0.7514	Cl–Cl	0.0415	0.1125	Br–Br	0.0411	0.0923
F–F	0.0492	0.2661	Cl–Cl	0.0663	0.1195	Br–Br	0.0496	0.0885
F–F	0.0232	0.1065	Cl–Cl	0.0060	0.0212	Br–Br	0.0172	0.0559
C–F	0.2355	-0.2841	C–Cl	0.1492	-0.0576	S–Br	0.0236	0.0666
S–F	0.0713	0.2306	S–Cl	0.0243	0.0730	S–Br	0.0121	0.0425
S–C	0.1498	-0.1520	S–C	0.1472	-0.1332	C–Br	0.1338	-0.0451

S–C	0.1582	-0.1765	S–C	0.1587	-0.1746	S–C	0.1482	-0.1357
S–C	0.1421	-0.1067	S–C	0.1468	-0.1362	S–C	0.1593	-0.1754
S–C	0.1547	-0.1545	S–C	0.1501	-0.1387	S–C	0.1452	-0.1313
S–C	0.1095	-0.0318	S–C	0.1194	-0.0516	S–C	0.1490	-0.1358
S–C	0.1615	-0.1669	S–C	0.1566	-0.1473	S–C	0.1227	-0.0579
						S–C	0.1547	-0.1420

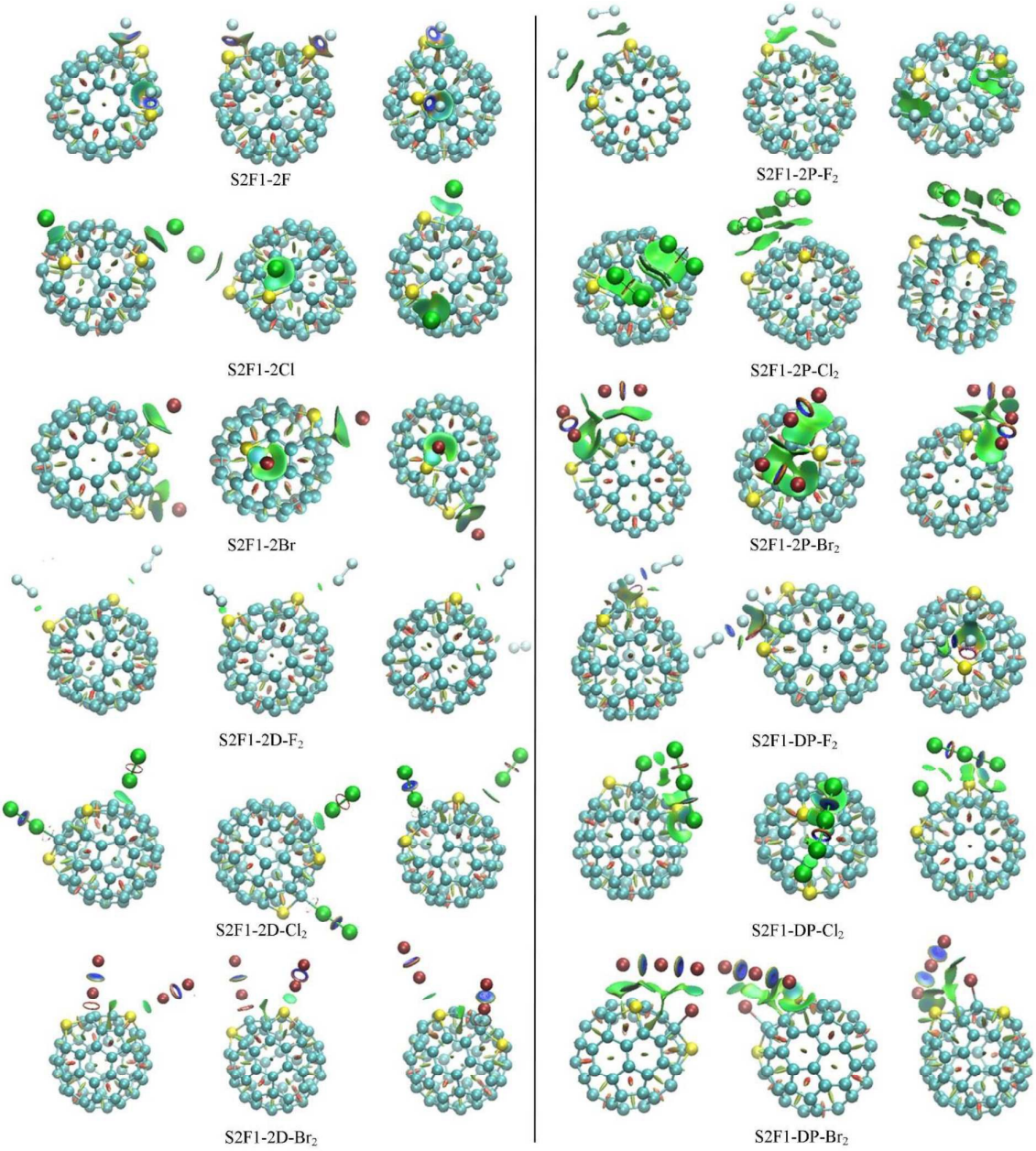

Fig. 6 Noncovalent interaction isosurfaces obtained from RDG and electron density frames for interactions of S2F1 model with halogens and halides

At the last step of this study, NCI index calculations were employed to produce noncovalent isosurfaces between absorbent and adsorbate species, which made additional evidence for being noncovalent interaction in our complexes. These type of calculations recently have developed as another proof for noncovalent interactions that sometimes produce different results from the QTAIM calculations.[50] The diagrams of isosurfaces (from several views for each model) for noncovalent interactions in S2F1 complexes were shown in figure 6 and for SF and S2F2 complexes were shown in supporting information (Figures S4 and S5). In addition, Figure 7 presents plots of sign $\lambda_2 \times \rho$ versus reduced density gradient (RDG) for all complexes.

In the above figure, green-colored isosurfaces show clearly noncovalent interaction by subtraction of RDG frames from electron density frames. According to NCIPLOT reference,[45] green isosurfaces represents a weak Van-der-Waals interaction between both sides of located species. Note that there is no

noncovalent interaction isosurface for one halogen atom in S2F1-DP-X_2 (X=F, Cl, Br) which refer to lack of such interaction in this case (and existing covalent bond). Although, there are much more troughs in negative area of electron density for S2F1-DP-X_2 (X=F, Cl, Br) complexes in figure 6 that could assign to more attractive interactions in those models.

RSC Advances

ARTICLE

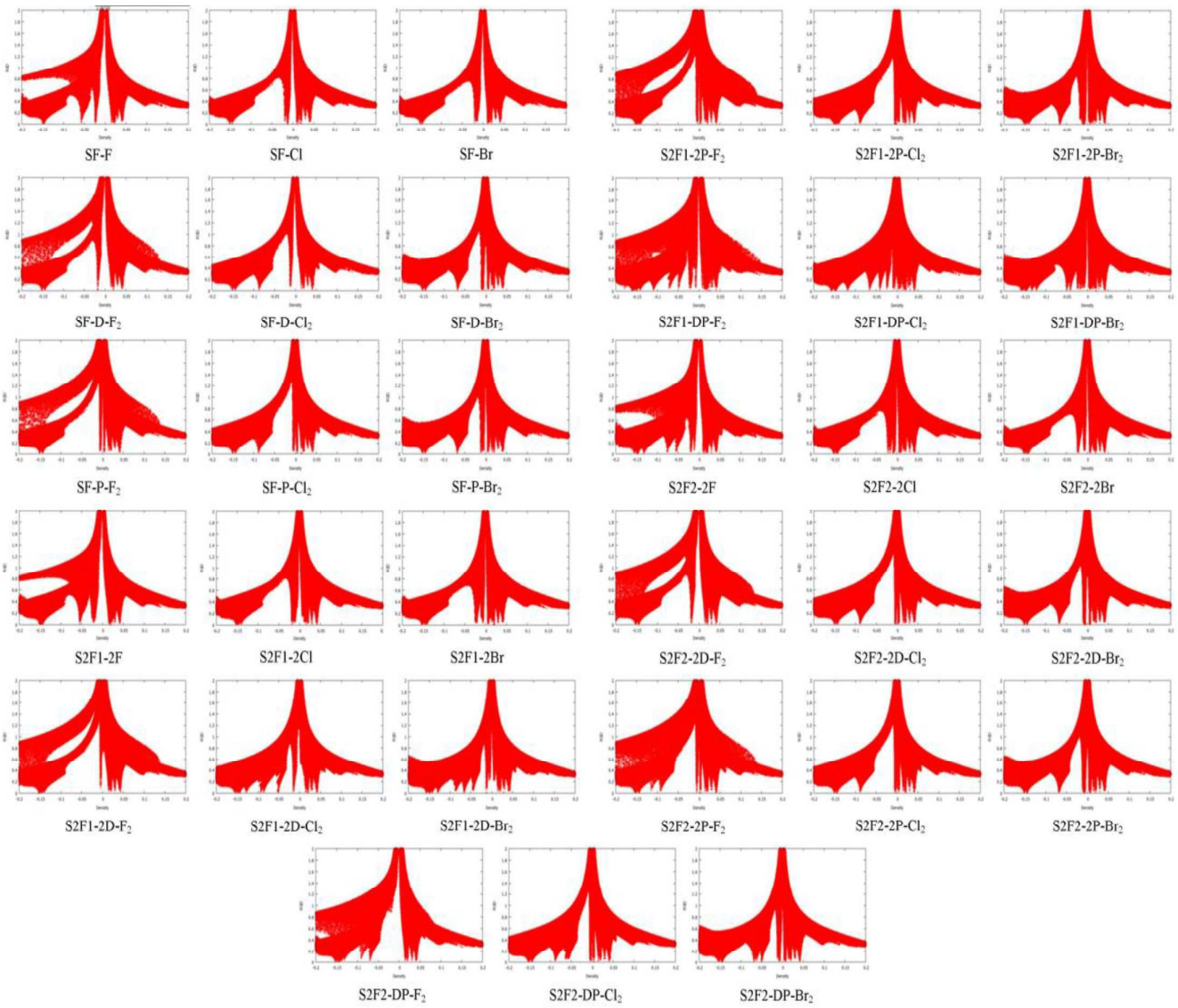

Fig. 7 Plots of sign $\lambda_2 \times \rho$ versus RDG of noncovalent interaction for all complexes

Conclusion

This theoretical study focused on noncovalent interaction of SFs with halogens and halides (exception of iodine) for possible sensor and adsorption application. Initiative SFs was chosen from optimized C_{60}-fullerene and by substitution of sulfur atom and locating halogens and halide on logical distances above fullerene's surface. Energy calculations showed that whole interactions are thermodynamically favorable, significantly in gaseous phase more than solvent phase. Among the solvents, in cyclohexane phase, interaction energy observed as the most favorable solvent and benzene and chloroform are placed in 2nd and 3rd orders, respectively. Moreover, the obtained data showed that chalcogen bond is the most important noncovalent interaction in these systems (with the highest interaction energies), the halogen bond stand at the 2nd place of importance and π-halogen bond is not existed in the most of these complexes. For S2F1-DP-X_2 (X=F,

Cl, Br) complexes, solvent phase shows more desirable media for interaction against gaseous phase that refers to this fact that mentioned complexes are more polar than their related initial structures. Donor-Acceptor interaction energies, obtained from NBO calculations, demonstrated direct effect of S-doping on acceptor species as long as σ^* C–S anticipated as most strengthen acceptor. However, more powerful transitions from lone-pair of carbon next to the doped sulfur to σ^* of halogens have been observed. NBO atomic charge revealed that doped sulfur atom has a large positive charge specially when interacting with halides and partial positive charge for neighborhood carbon atoms in doped site of fullerene. Investigation of DOS plots and population data leads to a decrease in E_g upon S-doping of fullerene, chemical hardness was tended to less values, global softness was increased and electrophilicity index was decreased. The least energy gap observed for S2F1 fullerene. QTAIM information indicated that these noncovalent interactions would be exists along absorbent and adsorbate for complexes with electrostatic interaction type. Interestingly, S2F1-DP-X_2 (X=F, Cl, Br) complexes have some other kind of interactions due to values of ρ and its negative Laplacian which stating likely partial functionalization of S2F1 fullerene because of its particular doping and special locating of halogens above it. It has proven that in these cases, the $[S2F1\text{-}X]^+X3^-$ stable structure could be produced from S2F1 and two molecular halogens via exothermic process. NCI index calculations confirmed the noncovalent interactions via depicted isosurfaces, and some toughs appeared in sign $\lambda_2 \times \rho$ versus RDG plots proof happening of electrostatic noncovalent interaction. Moreover, it is worthy to note that there is no noncovalent isosurface for one halogen atom that in binding with carbon atom next to doped sulfur atom in S2F2-X2 complexes.

Acknowledgements

We are grateful from High Performance Computing Research Center (HPCRC) at Amirkabir University of Technology, Tehran, Iran (National Amirkabir supercomputer; http://hpcrc.aut.ac.ir) and National High-Performance Computing Center (NHPCC) at Isfahan University of Technology (http://nhpcc.iut.ac.ir, Rakhsh supercomputer) for providing computational facilities to perform this work. This work has been supported by research affair of Isfahan University of technology

Notes and references

1 H. W. Kroto, J. R. Heath, S. C. O'Brien, R. F. Curl and R. E. Smalley, *Nature*, 1985, **318**, 162–163.
2 R. E. Smalley, *Acc. Chem. Res.*, 1992, **25**, 98–105.
3 M. S. Dresselhaus, G. Dresselhaus and P. C. Eklund, *Science of Fullerenes and Carbon Nanotubes*, Academic Press Ltd., 1996.
4 A. Mittelbach, W. Hönle, H. G. von Schnering, J. Carlsen, R. Janiak and H. Quast, *Angew. Chemie Int. Ed. English*, 1992, **31**, 1640–1642.
5 R. C. Haddon, A. F. Hebard, M. J. Rosseinsky, D. W. Murphy, S. J. Duclos, K. B. Lyons, B. Miller, J. M. Rosamilia, R. M. Fleming, A. R. Kortan, S. H. Glarum, A. V Makhija, A. J. Muller, R. H. Eick, S. M. Zahurak, R. Tycko, G. Dabbagh and F. A. Thiel, *Nature*, 1991, **350**, 320–322.
6 M. D. Diener and J. M. Alford, *Nature*, 1998, **393**, 668–671.
7 G. P. Tegos, T. N. Demidova, D. Arcila-Lopez, H. Lee, T. Wharton, H. Gali and M. R. Hamblin, *Chem. Biol.*, 2005, **12**, 1127–1135.
8 A. Jorio, G. Dresselhaus and M. S. Dresselhaus, Carbon Nanotubes: Advanced Topics in the Synthesis, Structure, Properties and Applications, Springer, 2007.
9 M. S. Dresselhaus and G. Dresselhaus, *Adv. Phys.*, 1981, **30**, 139–326.
10 Z. Wang, M. Yao, S. Pan, M. Jin, B. Liu and H. Zhang, *J. Phys. Chem. C*, 2007, **111**, 4473–4476.
11 S. Glenis, S. Cooke, X. Chen and M. M. Labes, *Chem. Mater.*, 1996, **8**, 123–127.
12 H. Jiao, Z. Chen, A. Hirsch and W. Thiel, *Phys. Chem. Chem. Phys.*, 2002, **4**, 4916–4920.
13 H. Tavakol and F. Hassani, *Struct. Chem.*, 2015, **26**, 151–158.
14 H. Tavakol and A. Mollaei-Renani, *Struct. Chem.*, 2014, **25**, 1659–1667.
15 P. A. Denis, R. Faccio and A. W. Mombru, *ChemPhysChem*, 2009, **10**, 715–722.
16 F. Hassani and H. Tavakol, *Sensors Actuators B Chem.*, 2014, **196**, 624–630.
17 E. G. Lewars, Computational Chemistry: Introduction to the Theory and Applications of Molecular and Quantum Mechanics Second Edition, Springer, 2011.
18 L. M. Azofra S. Scheiner, *J. Chem. Phys.* 2015, **142**, 034307.
19 X. Guo, X. An, Q. Li, *J. Phys. Chem. A* 2015, **119**, 3518−3527.
20 M. D. Esrafili, F. Mohammadian-Sabet, *Chem. Phys. Lett.* 2015, **628**, 71–75.
21 H. Tavakol, *J. Phys. Chem. A*, 2013, **117**, 6809–6816.
22 H. Tavakol, *Int. J. Quantum Chem.*, 2011, **111**, 3717–3724.
23 M. D. Ganji, N. Ahmadian, M. Goodarzi and H. A. Khorrami, *J. Comput. Theor. Nanosci.*, 8, 1392–1399.
24 Y. L. Wang, K. H. Su and J. P. Zhang, in *Advanced Materials Research*, Trans Tech Publ, 2012, vol. 463, pp. 1488–1492.
25 Z. J. Li, L. Wang, Y. J. Su and P. L. and Y. F. Zhang, *Nano-Micro Lett.*, 2009, **1**, 9–13.
26 H. Zeng, Z. Sun, Y. Segawa, F. Lin, S. Mao and Z. Xu, *Chem. Phys. Lett.*, 2001, **338**, 241–246.
27 H. Tavakol, *J. Mol. Struct. THEOCHEM*, 2010, **954**, 16–21.
28 H. Tavakol, M. Esfandyari, S. Taheri and A. Heydari, *Spectrochim. Acta Part A Mol. Biomol. Spectrosc.*, 2011, **79**, 574–582.
29 C. W. Bauschlicher Jr. and H. Partridge, *Chem. Phys. Lett.*, 1995, **240**, 533–540.
30 H. Tavakol, *Struct. Chem.*, 2011, **22**, 1165–1177.
31 H. Tavakol, *J. Mol. Struct. THEOCHEM*, 2010, **956**, 97–102.
32 H. Tavakol, *Mol. Simul.*, 2010, **36**, 391–402.
33 J.-D. Chai and M. Head-Gordon, *Phys. Chem. Chem. Phys.*, 2008, **10**, 6615–6620.
34 J.-D. Chai and M. Head-Gordon, *J. Chem. Phys.*, 2008, **128**, 084106.
35 J. Antony and S. Grimme, *Phys. Chem. Chem. Phys.*, 2006, **8**, 5287–5293.
36 S. Grimme, *J. Comput. Chem.*, 2006, **27**, 1787–1799.
37 J. Tomasi, B. Mennucci and R. Cammi, *Chem. Rev.*, 2005, **105**, 2999–3094.
38 G. E. S. M. J. Frisch, G. W. Trucks, H. B. Schlegel and many others, GAUSSIAN 09 (Revision A.02), Gaussian Inc., Wallingford, CT, 2009.
39 H. Tavakol and D. Shahabi, *J. Phys. Chem. C*, 2015, **119**, 6502–6510.

40 F. Weinhold and C. R. Landis, *Chem. Educ. Res. Pract.*, 2001, **2**, 91–104.
41 N. M. O'boyle, A. L. Tenderholt and K. M. Langner, *J. Comput. Chem.*, 2008, **29**, 839–845.
42 R. G. Parr, R. A. Donnelly, M. Levy and W. E. Palke, *J. Chem. Phys.*, 1978, **68**, 3801.
43 R. F. W. Bader, *Atoms In Molecules: A Quantum Theory*, Oxford University Press, 1990.
44 T. A. Keith, AIMAll, Version 10.05.04, TK Gristmill Software, Overland Park KS, USA, 2010.
45 E. R. Johnson, S. Keinan, P. Mori-Sanchez, J. Contreras-Garcia, A. J. Cohen and W. Yang, *J. Am. Chem. Soc.*, 2010, **132**, 6498–6506.
46 J. Contreras-García, E. R. Johnson, S. Keinan, R. Chaudret, J.-P. Piquemal, D. N. Beratan and W. Yang, *J. Chem. Theory Comput.*, 2011, **7**, 625–632.
47 W. Humphrey, A. Dalke and K. Schulten, *J. Mol. Graph.*, 1996, **14**, 33–38.
48 T. Williams, K. Colin and many others, gnuplot, version 4.6.5, http://www.gnuplot.info, 2014.
49 J. Cerny and P. Hobza, *Phys. Chem. Chem. Phys.*, 2007, **9**, 5291–5303.
50 J. R. Lane, J. Contreras-García, J.-P. Piquemal, B. J. Miller and H. G. Kjaergaard, *J. Chem. Theory Comput.*, 2013, **9**, 3263–3266.